Fuzzy Systems and Soft Computing
ISSN : 1819-4362

LOW COMPLEXITY DETECTOR WITH INDEX MODULATION FOR MIMO-OFDM SYSTEMS

Dr K Rajendra Prasad Assoc. Prof, ECE,
J.V Prabakar Rao Asst.Prof, ECE,
K L R College of Engineering and Technology, Palvancha, T.S, India :krpece.klr@gmail.com

Abstract
Multiple-input multiple-output orthogonal frequency division multiplexing with index modulation (MIMO-OFDMIM), which provides a flexible trade-off between spectral efficiency and error performance, is recently proposed as a promising transmission technique for energy-efficient 5G wireless communications systems. However, due to the dependence of subcarrier symbols within each subblock and the strong inter-channel interference, it is challenging to detect the transmitted data effectively while imposing low computational burden to the receiver. In this paper, we propose two types of low-complexity detectors based on the sequential Monte Carlo (SMC) theory for the detection of MIMO-OFDM-IM signals. The first detector draws samples independently at the subblock level while the second detector draws samples at the subcarrier level with further reduced complexity. To meet the constraint of the subcarrier combinations within each subblock, the second detector is further coupled with a carefully designed legality examination method. Attributed to the effectiveness of legality examination and deterministic SMC sampling, both proposed detectors achieve near-optimal error performance for the MIMO-OFDM-IM system.

Introduction

Increasing demand for higher spectral efficiency and reliability in the next generation wireless communications, multiple-input multiple-output (MIMO) systems have been receiving great attention for their ability in improving the transmission rate and error performance [1]– [3]. Recently, a novel MIMO scheme called spatial modulation (SM) has emerged as an appealing candidate to fulfill the spectral and energy efficiency requirements of the next generation wireless communication systems [4]–[10]. Owing to its various advantages, design and analysis of SM transmission in various scenarios, e.g., adaptive SM [11]–[13], generalized SM [14]–[16], and energy evaluation of SM [17]–[20], are extensively investigated.

Literature Survey

In [36] and [37], the optimal number of active subcarriers selection problem is investigated. In recent times, the performance of OFDM-IM is analyzed in terms of ergodic achievable rate [38] and average mutual information [39]. Due to the advantages of OFDM and MIMO transmission techniques, the combination of them has been regarded as a promising solution for enhancing the data rates of next generation wireless communications systems. More recently, by combining OFDM-IM with MIMO transmission techniques, a novel MIMO-OFDM with index modulation (MIMO-OFDMIM) scheme is presented in [40], which exhibits the potential to surpass the classical MIMO-OFDM. Specifically, by deactivating a subset of subcarriers, MIMO-OFDM-IM has the potential to achieve much better BER performance than classical MIMO-OFDM, resulting in higher energy efficiency for practical systems.
In this paper, in order to achieve near-optimal error performance while maintaining low computational complexity, two types of detection algorithms based on the sequential Monte Carlo (SMC) theory are proposed for MIMO-OFDM-IM. By regarding each OFDM-IM subblock as a super modulated symbol

drawn from a large finite set, the first type of detector draws samples independently at the subblock level. Although it is capable of achieving near-optimal performance with substantially reduced complexity, its decoding complexity can be still unsatisfactory when the size of the OFDM-IM subblock grows much larger. To further reduce the complexity, the second type of detector is proposed to draw samples subcarrierwise from the modified constellation with a much smaller size. Finally, computer simulation and numerical results in terms of BER and number of complex multiplications (NCM) corroborate the superiority of both proposed detection methods.

The Basis of OFDM system

In an OFDM system, there are mainly two components, transmitter and receiver. Each component has several steps to process the signal in order to properly transmit the data from the transmitter to the receiver. Fig. 2.1 illustrates is a block diagram of a typical OFDM communication system.

The source data are a sequence of binary bits, for example, 11100100. The incoming bit stream of 1s and 0s is multiplexed into N parallel bit streams. Then, the N parallel bit stream are

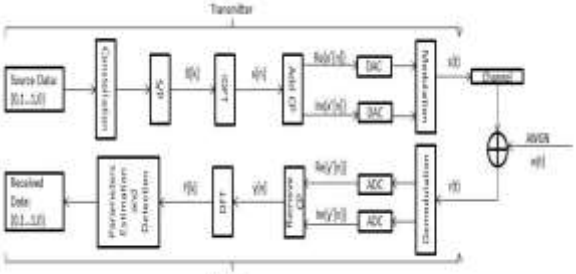

Fig 2. 1 Block Diagram of OFDM system

independently mapped in the frequency domain into complex symbols, denoted by X[k], in a given constellations such as phase shift Keying (PSK) or quadrature amplitude modulation (QAM), [37].

PSK is a digital modulation scheme that transfers the source data by modulating the phase of the carrier (or subcarriers), which uses a finite number of phases, each assigned to a unique pattern of data bits. Usually, each phase encodes an equal number of bits. Each pattern of bits forms the symbol that is represented by the particular phase. Fig. 2.2 shows the constellation diagram for 4-PSK modulation.

Hermetian symmetry

After having mapped the N channels it is applied the Hermetian symmetry so that the modulation can be made by an IFFT. It is generated 2N+2 channels in symmetry.In the receiver, to the end of the processing of FFT, they are sent to the decoder only N channels, being eliminated the channels generated due to Hermetian symmetry.

The Hermetian symmetry is implemented in agreement with

$$X_0 = X_{\overline{N}} = 0$$
$$X_k = d_k$$
$$X_{2\overline{N}-k} = d_k^*$$

for k = 1, 2..., N - 1, where N = N +1.

k	X_k	X_{8-k}
1	$X_1 = d_1$	$X_7 = d_1^*$
2	$X_2 = d_2$	$X_6 = d_2^*$
3	$X_3 = d_3$	$X_5 = d_3^*$

For instance, to transmit N = 3 channels (d1, d2, d3) N = 4, 2N = 8 and k = 1, 2, 3. Applying in

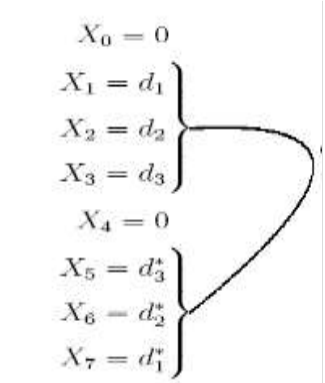

the above equation it is obtained the result shown in the following table.

In that way, it can stay X0 and XN always in zero. While it is made XN+1 even X_{2n-i} same to the conjugated of X_{n-1}.Being it conjugated of Z = a+jb the same of Z* = a- jb, then to do the operation of having conjugated he should move the sign of the imaginary part, in other words, to do a sign inversion. In hardware, the inversion of sign of a binary number in complement two.

MIMO-OFDM-IM

In this paper, we consider a MIMO-OFDM-IM system equipped with Nt transmit and Nr receive antennas [40], [41]. The block diagram of the MIMO-OFDM-IM transmitter is depicted in Fig. 1. Each MIMO-OFDM-IM frame is comprised of a total number of mNt incoming data bits. These bits are divided into Nt groups for Nt transmit antennas, each of which contains m bits for the generation of an OFDM-IM block to be transmitted from a transmit antenna. These m bits are further divided into G subgroups, each of which consists of p bits, i.e., m = Gp. Assuming NF available subcarriers of each block, each subgroup is then used to generate an OFDM-IM subblock consisting of N = NF /G subcarriers. Unlike classical OFDM, which maps all data bits to the constellation points for all subcarriers, OFDM-IM separates p bits of each subblock into two parts for different purposes: the first part with p1 = blog2 N K c bits is used to select K actisubcarriers, while the remaining N − K subcarriers are set to be idle;1 the second part with p2 = K log2 M bits is mapped into K modulated symbols for the K active subcarriers via M-ary modulation. The mapping between the p1 bits and the subcarrier combination patterns can be implemented by using a look-up table or the combinatorial method [26]. Consider the g-th ($1 \le g \le G$) OFDM-IM subblock at the t-th ($1 \le t \le Nt$) transmit antenna. Accordingly, the output of the first part should be the indices of K active subcarriers, which are given by the following set:

J g t = {j g t (1), . . . ,jg t (K)} (1)

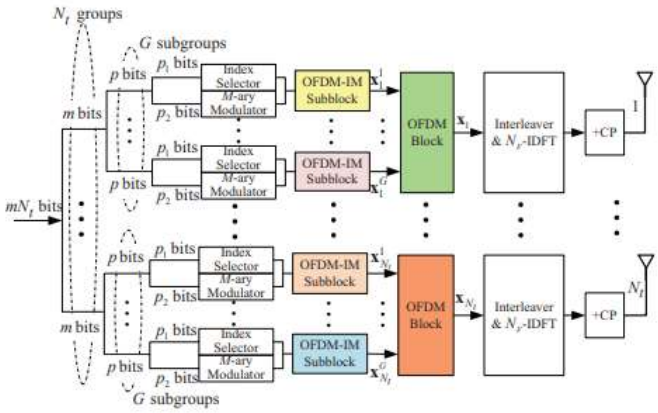

Fig Block diagram of MIMO-OFDM-IM transmitter.

where j g t (k) ∈ {1, . . . , N} for k = 1, . . . , K, and the elements of J g t are sorted in an ascending order, i.e., j g t (1) < j g t (2) < · · · <jg t (K). The output of the second part should be K modulated symbols {s g t (n)}n∈J g t , where s g t (n) is drawn from a complex alphabet S˜ with |S| ˜ = M and we assume that E |s g t (n)| 2 = 1 for the normalization of signal constellation. Therefore, the g-th OFDM-IM subblock element at the t-th transmit antenna can be expressed as x g t = [x g t (1) x g t (2) · · · x g t (N)]T , where From above, it is clear that each subblock of the MIMOOFDM-IM contains a fixed number of active subcarriers, whose positions carry information through the subcarrier indices. After generating all OFDM-IM subblocks, each OFDM-IM block is created by concatenating G OFDM-IM subblocks in each branch of the transmitter, which is denoted by xt = h x 1 t T x 2 t T · · · x G t TiT , [xt(1) xt(2) · · · xt(NF)]T , where 1 ≤ t ≤ Nt. To fully benefit from the frequencyselective fading, a G × N block interleaver (a.k.a. OFDM-IM with interleaved grouping in [29], [38]) is employed in each branch of the transmitter. Before transmission, each OFDMIM block is first transformed into the time-domain signal block by employing an NF -point inverse discrete Fourier transform (IDFT), and then appended with a CP of length Ncp, which is longer than the maximum delay spread of the channel. The spectral efficiency of MIMO-OFDM,

(3) As shown in Fig. Furthermore, for the n-th (1 ≤ n ≤ N) subcarrier of the g-th (1 ≤ g ≤ G) OFDM-IM subblock, the signal vector observed at the receiver can be collected as

$$\underbrace{\begin{bmatrix} y_1^g(n) \\ y_2^g(n) \\ \vdots \\ y_{N_r}^g(n) \end{bmatrix}}_{\mathbf{y}_n^g} = \sqrt{\frac{\rho}{N_t}}\sqrt{\frac{N}{K}} \underbrace{\begin{bmatrix} h_{1,1}^g(n) & h_{1,2}^g(n) & \cdots & h_{1,N_t}^g(n) \\ h_{2,1}^g(n) & h_{2,2}^g(n) & \cdots & h_{2,N_t}^g(n) \\ \vdots & \vdots & \ddots & \vdots \\ h_{N_r,1}^g(n) & h_{N_r,2}^g(n) & \cdots & h_{N_r,N_t}^g(n) \end{bmatrix}}_{\mathbf{H}_n^g} \times \underbrace{\begin{bmatrix} x_1^g(n) \\ x_2^g(n) \\ \vdots \\ x_{N_t}^g(n) \end{bmatrix}}_{\mathbf{x}_n^g} + \underbrace{\begin{bmatrix} w_1^g(n) \\ w_2^g(n) \\ \vdots \\ w_{N_r}^g(n) \end{bmatrix}}_{\mathbf{w}_n^g} \quad (5)$$

where y¯ g n is the received signal vector, H g n is the corresponding channel matrix which contains the CFRs between the transmit and receive antennas at the n-th subcarrier, x¯ g n is the data vector which contains the simultaneously transmitted symbols from all transmit antennas at the n-th subcarrier, and w¯ g n is an Nr × 1 AWGN vector whose elements have zero mean and unit variance. where Ag n = H¯ g n H H¯ g n , and w˜ g n = (Ag n) −1/2 H¯ g n H w¯ g n is an Nt ×1 AWGN vector whose

elements have zero-mean and unit variance. Let us stack the received signal vectors in (6) for N consecutive subcarriers of the g-th ($1 \leq g \leq G$) OFDM-IM subblock.

SMC and sequential Structure For MIMO-OFDM

The SMC method, also referred to as particle filter, is a class of the sampling based sequential Bayesian inference methodologies for general dynamic systems, which has been widely applied in wireless communications [43]–[48]. In the following, we will first briefly introduce the concept of the deterministic SMC and then construct the sequential structure for MIMO-OFDM.

Sequential Structure for MIMO-OFDM-IM

To apply the SMC theory to the detection of MIMOOFDM-IM, we construct the sequential structure based on the observed signals in the sequel. Inspired by the successive interference cancellation (SIC) method for the MIMO detection [49], we apply the QL decomposition3 to the matrix (Ag n) 1/2 in (6) as (Ag n) 1/2 = QgnL g n , n = 1, . . . , N, g = 1, . . . , G (9)

where Qg n is a unitary matrix, and L g n is a lower triangular matrix. The lower triangular operation is carried out by the left multiplication of the vector y˜ g n in (6) by (Qgn) H to obtain z¯ g n = (Qg n) H y˜ g n , which can be further written as where v¯ g n = (Qgn) H w˜ g n is still an Nt × 1 zero-mean AWGN vector with unit variance elements as the matrix Qg n is unitary. Based on the structure in (10), the SIC may be applied to detect the data vector x¯ g n in a sequential manner, i.e., the interference due to the previously decoded symbols is subtracted from the observed sample before decoding the next symbol. However, one should keep in mind that unlike the classical MIMO-OFDM in which the symbols carried on the different subcarriers are independently generated, the symbols carried on different subcarriers within each OFDMIM subblock are binded together in the MIMO-OFDM-IM due to the index modulation. Therefore, to be suited to MIMOOFDM-IM, the SIC method for MIMO-OFDM-IM has to be performed in a subblock-by-subblock manner, resulting in a search complexity as high as of order NtNCMK. Moreover, the SIC method may suffer from the problem of error propagation, which also limits its error performance. In this paper, we will not employ the SIC method but instead exploit the aforementioned sequential structure for the low-complexity detector design of MIMO-OFDM-IM.

LOW-COMPLEXITY DETECTORS FORMIMO-OFDM-IM

In this section, we will develop two types of SMC-based detectors by using the structure of (10) as the kernel for MIMOOFDM-IM. As will be shown by computer simulations, the new algorithms can avoid error propagation successfully and provide near-optimal error performance for MIMO-OFDMIM.

A. Deterministic SMC Aided Subblock-wise Detection

After the lower triangular operation, the sequential structure in (10) can be exploited by applying the SMC method to draw samples starting from the first transmit antenna and ending to the last one. Indeed, if we simply regard each OFDM-IM subblock x g t as a super modulated symbol drawn from a large finite set, we have the a posteriori distribution of {x g t } Nt t=1 conditioned on {z g t } Nt t=1 as where z g t , [z g t (1) z g t (2) · · · z g t (N)]T denotes the observed subblock in the t-th ($1 \leq t \leq Nt$) branch of the receiver after the lower triangular operation in (10), and X g t , {x g t 0} t t 0=1. Based on (11), we construct the sequence of probability distributions n P X g t Z g t oNt t=1 , which can be expressed as where Z g t , {z g t 0} t t 0=1. From the perspective of the probability theory, our aim is to estimate the a posteriori probability of each OFDM-IM subblock. based on the observed subblocks {z g t }Nt t=1, where Φ˜ , {Φi} NCMK i=1 with |Φ˜ | = NCMK denotes the set including all possible realizations of the OFDM-IM subblock. Instead of the direct computation of (13), which is too computationally expensive,

we seek to numerically approximate (13) by using the deterministic SMC theory to substantially reduce the complexity at the receiver. Let (X g t) (b) with b = 1, . . . , β be the particles drawn by the SMC method at the t-th sampling interval on the basis of subblock, where β denotes the total number of particles. To implement the SMC method, we first generate a set of incomplete particles for the OFDM-IM subblocks, and then update the corresponding importance weights for those particles with respect to the distribution of (11) until the subblock at the last antenna is reached. Moreover, to update the importance weights, it is crucial to design the trial distribution which minimizes the variance of the importance weights conditioned upon the previous particles and the observed signals [50]. Under the criterion of minimum conditional variance of the importance weights, we simply choose the trial distribution as for t = 1,, Nt. Proposition 1: With the trial distribution given in (14), the importance weight for the SMC can be updated according 5) where p z g t X g t−1 (b) can be regarded as the prediction distribution of the current observed subblock z g t under the condition of the previous particle X g t−1.

Algorithm 1 Deterministic SMC aided subblock-wise detection

1: Perform the lower triangular operation to obtain (10);
2: Enumerate all possible realizations of $\mathbb{X}_\Gamma^g$ with their *a posteriori* probabilities given in (21), and retain the β initial particles $\left\{(\mathbb{X}_\Gamma^g)^{(b)}\right\}_{b=1}^{\beta}$ with the highest *a posteriori* probabilities as the initial importance weights $\left\{(\varpi_\Gamma^g)^{(b)}\right\}_{b=1}^{\beta}$;
3: **for** $t = \Gamma + 1$ to N_t **do**
4: Update the importance weights according to (18), $b = 1, \ldots, \beta$;
5: Pick up and retain β particles with the highest importance weights among the $\beta|\tilde{\mathbf{\Phi}}|$ hypotheses with weights set $\left\{(\varpi_t^g)_{[i]}^{(b)}\right\}$, $b = 1, \ldots, \beta$, $i = 1, \ldots, N_C M^K$;
6: **end for**
7: Compute the *a posteriori* probability for each subblock via (22), and the estimate of each subblock is given by $\widehat{\mathbf{x}}_t^g = \arg\max_{\mathbf{\Phi}_i \in \tilde{\mathbf{\Phi}}} P\left(\mathbf{x}_t^g = \mathbf{\Phi}_i \middle| \{\mathbf{z}_t^g\}_{t=1}^{N_t}\right)$, $t = 1, \ldots, N_t$.

Table. Deterministic SMC aided sub block wise detection

Initialization and Summary of Subblock-Wise Agorithm: By assuming the SMC process starts at the Γ-th transmit antenna, we compute the a posteriori distributions P X g Γ Z g Γ exactly by enumerating all possible realizations of X g Γ , where the total number of possible realizations is |Φ˜ | Γ and Γ < Nt. 4 According to the deterministic SMC and (10), the a posteriori probabilities P (X g Γ) (b) Z g Γ can be ex . (21) where b = 1, . . . , BΓ, BΓ = |Φ˜ | Γ, and n (X g Γ) (b) oBΓ b=1 contains all possible realizations of X g Γ . Then we retain the β particles n (X g Γ) (b) oβ b=1 with the highest a posteriori probabilities as the initial importance weights n ($ g Γ) (b) oβ b=1 , where β ≤ BΓ. After the initialization, the importance weights are updated according to (18). At each sampling interval on the basis of subblock, current β particles with the highest importance weights are selected as the survivors over β|Φ˜ | possible hypotheses departed from the previous particles.

Deterministic SMC Aided Subcarrier-wise Detection Although the detector proposed in Section IV-A achieves considerable reduction in computational complexity with respect to the ML detector, its complexity still grows exponentially with the size of subblock. To circumvent this problem, we propose

another novel detection algorithm based on the deterministic SMC in this subsection, which draws samples at the subcarrier level. To prevent from outputting illegal subblock realization, the subcarrier-wise detector takes into account the constraint of the active subcarrier combinations within each subblock when drawing samples. By exploiting the sequential structure in (10), the subcarrier-wise SMC method detects the information starting from the first transmit antenna and ending to the last transmit antenna and draws samples subcarrier-wise from the first subcarrier to the last subcarrier within the g-th subblock at each transmit antenna . Unlike the detector proposed in Section IV-A that estimates the information subblock-wise, the aim of the subcarrier-wise detection is to estimate the a posteriori probability at the subcarrier level, which is given by with |X | ˜ = M + 1 denotes the modified constellation. However, due to the dependence of subcarrier symbols within each subblock, it is infeasible to compute (26) directly. Therefore, we resort to the SMC theory by carefully considering this dependent relationship. Suppose that Xegt,n(b) with b = 1, . . . , β are the particles drawn by the SMC method at each sampling interval on the basis of subcarrier.

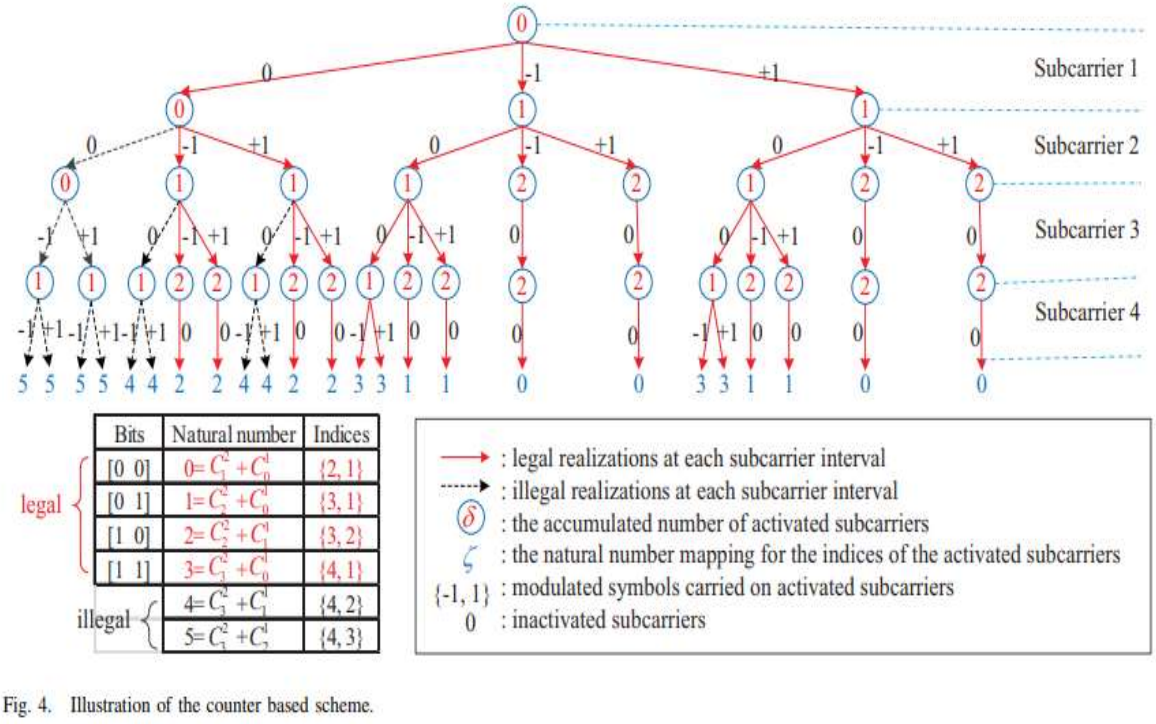

Fig. 4. Illustration of the counter based scheme.

Fig 5. 1 Counter based scheme.

1) **Exhaustive Searching Scheme:** According to the Bayes theorem, we can obtain the conditional probability exactl (33) where Φi = [Φi(1) Φi(2) · · · Φi(N)]T . According to (33), if the hypothesis n x g t,n−1 (b) , Xi o is illegal, we will have P x g t (n) = Xi x g t,n−1 (b) = 0, such that, the illegal hypotheses can be avoided. However, it is costly to calculate the conditional probability exactly based on (33) as it invokes an exhaustive search over all possible realizations of the OFDM-IM subblock at every sampling interval on the basis of basis of subcarrier.

2) Natural Numbers Mapping Scheme: To strike a tradeoff between the complexity cost and the estimation accuracy, we hereafter develop a more efficient method to estimate the conditional probability in (33) and to avoid the propagation of illegal particles. Let us denote the number of non-zero elements in x g t,n−1 as δ (b) n−1 = count x g t,n−1 (b) . Assuming that subcarriers within a subblock are uniformly activated and the modulated symbols are uniformly drawn from an M-ary

constellation, we can estimate the conditional pro i = 0 (34) where t = 1, . . . , Nt, n = 1, . . . , N, and i = 1, . . . , M + 1. Based on (34), x g t,N (b) with t = 1, . . . , Nt after the SMC sampling procedure are forced to meet the fixed number constraint of active subcarriers within each subblock, i.e., δ (b) N = K for b = 1, . . . , β. It is worth pointing out that the calculation of (34) does not involve any specific mapping rule for the subcarrier combination, which is more general and practical. However, when NC 6= N K , the calculation of (34) will encounter the infiltration of some illegal realizations, i.e., the conditional probabilities of some illegal realizations are not zero. To detect those illegal realizations without using a look-up table, we resort to the combinatorial method in [26] to examine the legality of the realization. The method in [26] provides a one-to-one mapping between natural numbers and the combination patterns of K active subcarriers, which is given by ζ = j(K) − 1 K + · · · + j(2) − 1 2 + j(1) − 1 1 (35) where t and g are omitted as (35) is general for all subblocks, and 0 ≤ ζ ≤ N K − 1. Based on (35), we can easily examine the legality of the realizations by simply regarding those realizations with ζ ≥ NC as illegal. Example 1: Suppose BPSK modulation, N = 4 and K = 2 and the combinatorial method is applied to determine the indices of the two active subcarriers out of four available subcarriers, as shown in the table in Fig. 4. The graphical tree is also illustrated in Fig. 4 according to (34). As can be seen, based on (35), we can easily exclude those illegal realizations with ζ ≥ 4. For the calculation based on (34), it can be readily verified that the ratio of the number of the illegal realizations to that of legal ones is N K − NC /NC , which is typically small. For this reason, we only examine the legality of the particles when they reach the last subcarrier within each subblock, i.e., n = N. Remark: As illustrated above, the method based on (34) and (35) does not require any look-up table and is general for different N and K values, which is more efficient and practical than the calculation based on (33). Owing to its simplicity and generality, the calculation based on (34) and (35) will be adopted to estimate the conditional probability P x g t (n) = Xi x g t,n−1 (b) in (29) for our computer simulations in Section.

3) Initialization and Summary of Subcarrier-Wise Algorithm: We assume that the SMC process starts on the Λ-th subcarrier of the subblock at the Γ-th transmit antenna and enumerate all legal realizations of XegΓ,Λ , where Γ ≤ Nt, Λ ≤ N, and the total number of legal realizations is BeΓ,Λ ≤ |Φ˜ | Γ−1 |X | ˜ Λ. 5 According to the deterministic SMC and (10), we can enumerate all legal realizations of Xeg Γ,Λ and compute their a posteriori probabilities exactly Λ. After the initialization, we update the importance weight according to (29). At each sampling interval on the basis of subcarrier, current β particles with the highest importance weights are selected as the survivors over β|X | ˜ = β (M + 1) possible hypotheses departed from the previous particles. Specially, when the recursion reaches the last subcarrier of each subblock, i.e., n = N, the legality of the possible samples will be first examined according to (35) and β legal particles with the highest importance weights are selected as the survivors over those legal hypotheses. When the recursion reaches the bottom, i.e., t = Nt and n = N, the particles associated with the importance weights are then used to compute the a posteriori probability for each subcarrier symbol in (26), g where Xi ∈ X˜ and $e g Nt,N = Pβ b=1 $ g Nt,N (b) . However, as emphasized above, due to the dependence of subcarriers within each subblock, we cannot estimate each symbol independently based on (37) as the demapping of OFDM-IM subblock may fail. Simply, by considering the joint estimation for active subcarriers and modulated symbols within each subblock, we can estimate the a posteriori probability for each subblock similar to (22) to solve this problem.

Algorithm 2 Deterministic SMC aided subcarrier-wise detection

Perform the lower triangular operation to obtain (10);
Enumerate all legal realizations of $\widetilde{\mathbf{X}}^q_{\Gamma,\Lambda}$ with their *a posteriori* probabilities given in (36), and retain the β initial particles $\left\{\left(\widetilde{\mathbf{X}}^q_{\Gamma,\Lambda}\right)^{(b)}\right\}_{b=1}^{\beta}$ with the highest *a posteriori* probabilities as the initial importance weights $\left\{\left(\varpi^q_{\Gamma,\Lambda}\right)^{(b)}\right\}_{b=1}^{\beta}$;
for $n = \Lambda + 1$ to N **do**
  Update and examine the particles associated with the importance weights according to (29) and (35), $b = 1, \ldots, \beta$;
end for
for $t = \Gamma + 1$ to N_t **do**
  for $n = 1$ to N **do**
    Update the importance weights according to (29), $b = 1, \ldots, \beta$;
    if $n = N$ **then**
      Compute ζ mapping for the K active subcarrier indices extracted from each hypothesis $\left\{\left(\varpi^q_{t,N-1}\right)^{(b)}, \mathcal{X}_i\right\}$ according to (35), and set the importance weights for those illegal hypotheses ($\zeta \geq N_C$) to zero, $b = 1, \ldots, \beta$, $i = 1, \ldots, M+1$;
    end if
    Pick up and retain β particles with the highest importance weights among the $\beta|\widetilde{\mathcal{X}}| = \beta(M+1)$ hypotheses with the set of weights $\left\{\left(\varpi^q_{t,n}\right)^{(b)}_{|i|}\right\}$, $b = 1, \ldots, \beta$, $i = 1, \ldots, M+1$;
  end for
end for
Compute the *a posteriori* probability for each subblock via (38), and the estimate of each subblock is given by $\widehat{\mathbf{x}}^q_t = \arg\max_{\mathbf{\Phi}_i \in \mathbf{\Phi}} P\left(\mathbf{x}^q_t = \mathbf{\Phi}_i \middle| \{\mathbf{z}^q_t\}_{t=1}^{N_t}\right)$, $t = 1, \ldots, N_t$.

Table. Deterministic SMC aided subcarrier - wise detection

Simulation Results

Comparison Fig. 5 shows the BER comparison results of different detection algorithms for the MIMO-OFDM-IM system with Nt = 4, K = 1, and QPSK modulation. As seen from Fig. 5, the proposed subblock-wise detector achieves nearoptimal BER performance for the MIMO-OFDM-IM system with reduced complexity for both N = 2 and N = 4 cases. BER comparison results of different detection algorithms for the MIMO-OFDM-IM system with Nt = 4, N = 4, and BPSK modulation. It can be observed that similarly the proposed subblock-wise detector achieves near-optimal performance while the proposed subcarrier-wise detector only suffers from a marginal performance loss compared to the ML detection. Although the MMSE-LLR-OSIC detector outperforms the other two MMSE based detectors at the cost of a higher complexity, its performance is still far from optimal (ML detection). By comparing the two scenarios with different number of active subcarriers (K = 1. observe that the BER performance of all detectors degrades as the number of active subcarriers increases. This can be understood as each active subcarrier will be allocated less power when more subcarriers are activated simultaneously for transmission.

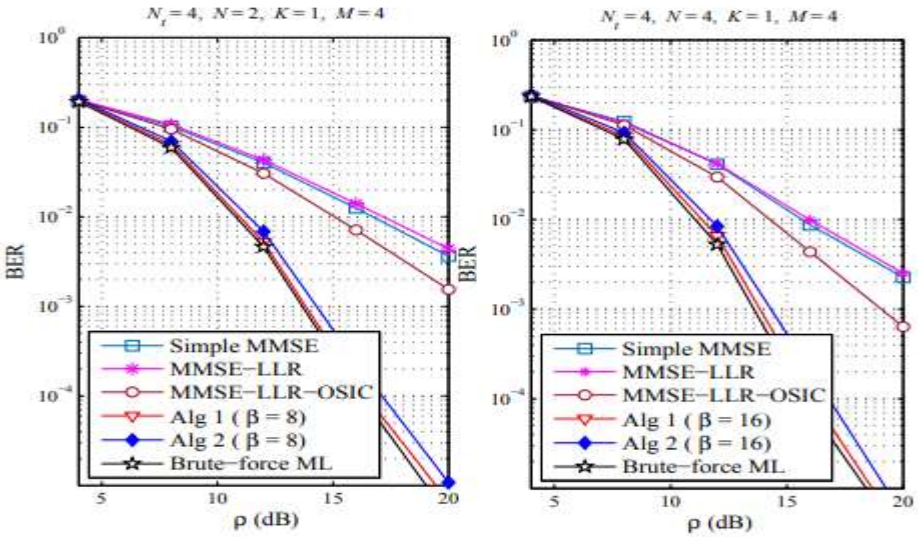

Fig BER performance comparison of different detection algorithms for MIMO-OFDM-IM with Nt = 4, K = 1, and QPSK modulation

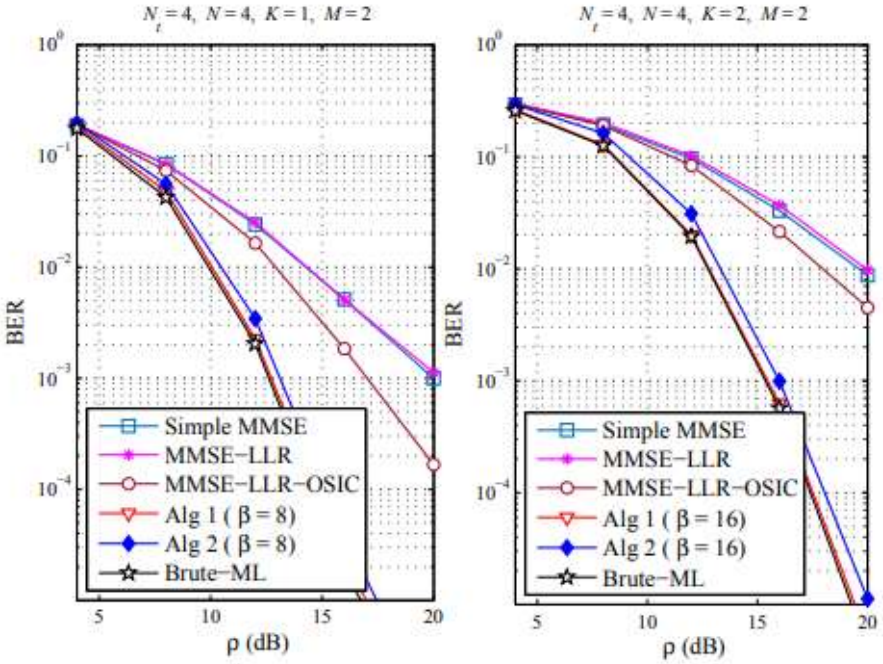

Fig BER performance comparison of different detection algorithms for MIMO-OFDM-IM with Nt = 4, N = 4, and BPSK.

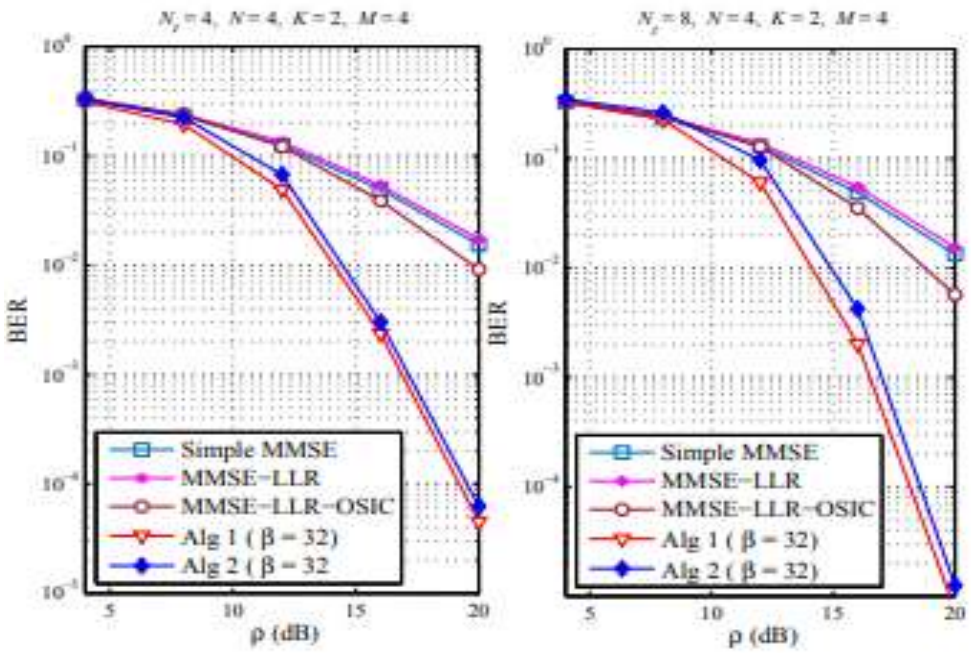

Fig BER performance comparison of different detection algorithms for MIMO-OFDM-IM with N = 4, K = 2, and QPSK modulation.

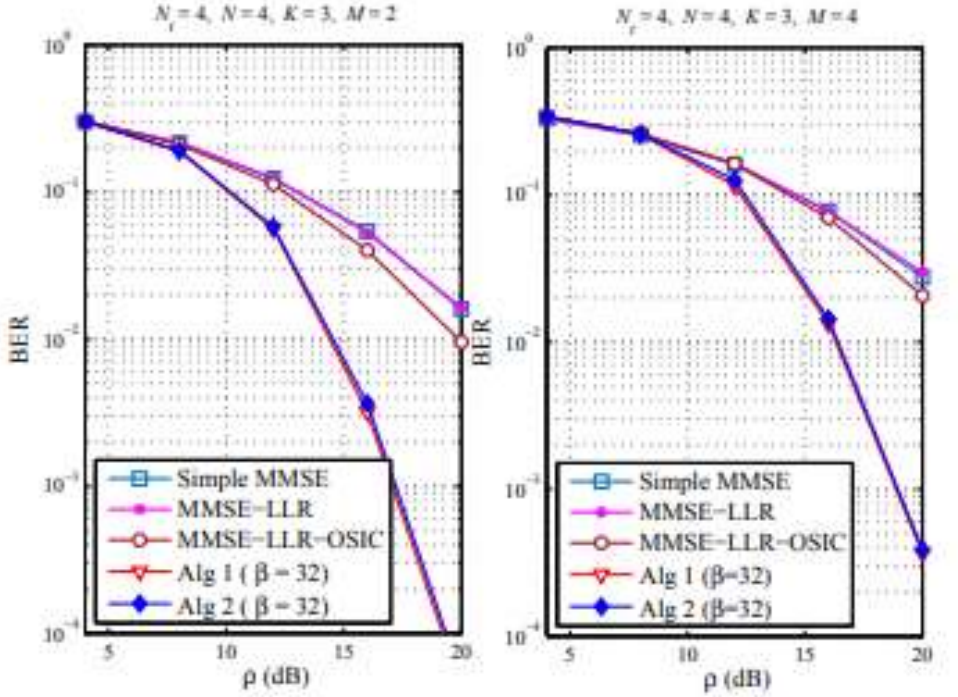

Fig BER performance comparison of different detection algorithms for MIMO-OFDM-IM with Nt = 4, N = 4, and K = 3

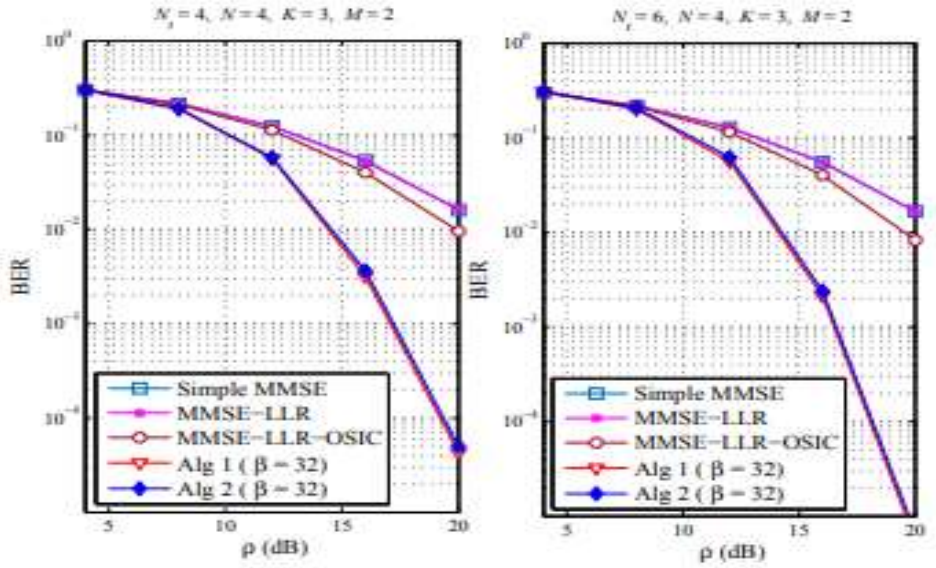

Fig BER performance comparison of different detection algorithms for MIMO-OFDM-IM with N = 4, K = 3, and BPSK modulation

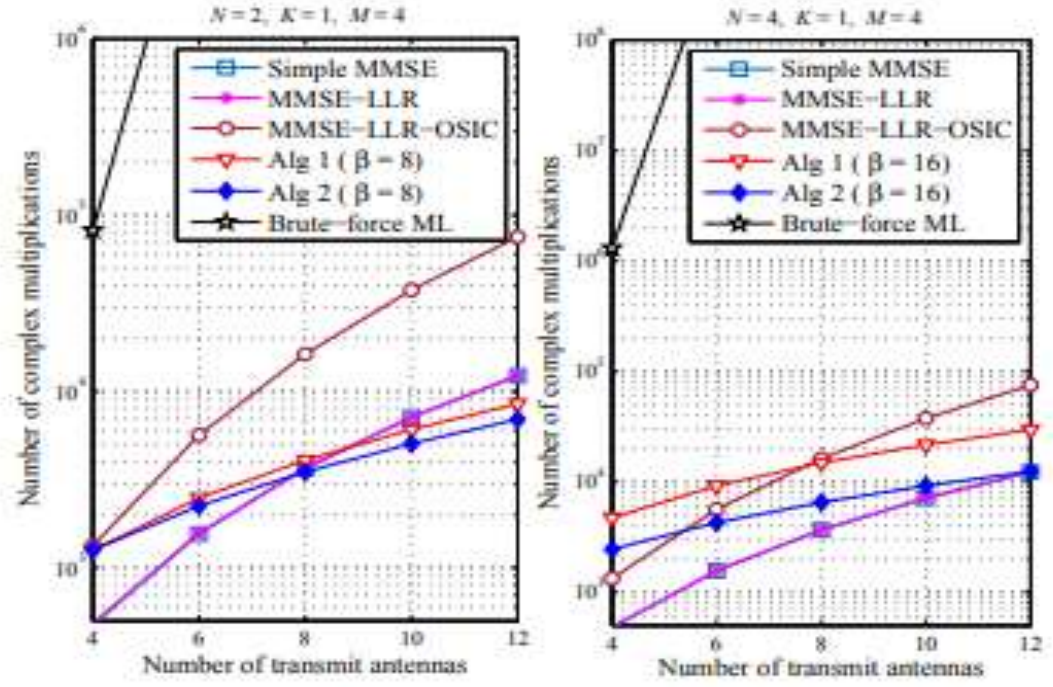

Fig.Complexity comparison of different detection algorithms for MIMOOFDM-IM with K = 1, and QPSK modulation.

Conclusion

In this paper, we have proposed two low-complexity detectors derived from the SMC theory for the MIMO-OFDMIM system. The first proposed subblock-wise detector draws samples at the subblock level, exhibiting near-optimal performance for the MIMO-OFDM-IM system. The second proposed subcarrier-wise detector draws samples at the subcarrier level, exhibiting substantially reduced

complexity with a marginal performance loss. An effective legality examination method has been also developed to couple with the subcarrierwise detector. Computer simulation and numerical results have validated the outstanding performance and the low complexity of both proposed detectors.

REFERENCES

[1] M. U. Celik, G. Sharma, A. M. Tekalp, and E. Saber, "Lossless generalized-LSB data embedding," IEEE Trans. Image Process., vol. 14, no. 2, pp. 253–266, Feb. 2005. [2] M. U. Celik, G. Sharma, and A. M. Tekalp, "Lossless watermarking for image authentication: A new framework and an implementation," IEEE Trans. Image Process., vol. 15, no. 4, pp. 1042–1049, Apr. 2006.

[3] Z. Ni, Y.-Q. Shi, N. Ansari, and W. Su, "Reversible data hiding," IEEE Trans. Circuits Syst. Video Technol., vol. 16, no. 3, pp. 354–362, Mar. 2006.

[4] X. Li, W. Zhang, X. Gui, and B. Yang, "A novel reversible data hiding scheme based on two-dimensional difference-histogram modification," IEEE Trans. Inf. Forensics Security, vol. 8, no. 7, pp. 1091–1100, Jul. 2013.

[5] C. Qin, C.-C.Chang, Y.-H.Huang, and L.-T. Liao, "An inpaintingassisted reversible steganographic scheme using a histogram shifting mechanism," IEEE Trans. Circuits Syst. Video Technol., vol. 23, no. 7, pp. 1109–1118, Jul. 2013.

[6] W.-L. Tai, C.-M.Yeh, and C.-C. Chang, "Reversible data hiding based on histogram modification of pixel differences," IEEE Trans. Circuits Syst. Video Technol., vol. 19, no. 6, pp. 906–910, Jun. 2009.

[7] J. Tian, "Reversible data embedding using a difference expansion," IEEE Trans. Circuits Syst. Video Technol., vol. 13, no. 8, pp. 890–896, Aug. 2003.

[8] Y. Hu, H.-K. Lee, and J. Li, "DE-based reversible data hiding with improved overflow location map," IEEE Trans. Circuits Syst. Video Technol., vol. 19, no. 2, pp. 250–260, Feb. 2009.

[9] X. Li, B. Yang, and T. Zeng, "Efficient reversible watermarking based on adaptive prediction-error expansion and pixel selection," IEEE Trans. Image Process., vol. 20, no. 12, pp. 3524–3533, Dec. 2011.

[10] X. Zhang, "Reversible data hiding with optimal value transfer," IEEE Trans. Multimedia, vol. 15, no. 2, pp. 316–325, Feb. 2013.

[11] T. Bianchi, A. Piva, and M. Barni, "On the implementation of the discrete Fourier transform in the encrypted domain," IEEE Trans. Inf. Forensics Security, vol. 4, no. 1, pp. 86–97, Mar. 2009.

[12] T. Bianchi, A. Piva, and M. Barni, "Composite signal representation for fast and storage-efficient processing of encrypted signals," IEEE Trans. Inf. Forensics Security, vol. 5, no. 1, pp. 180–187, Mar. 2010.

s/crypto.pdf.